Temperature Distribution and Numerical Modeling of Heat Transfer in Block 276 P1-Sand – Part I

R. Trabelsi[1*], A. C. Seibi[2], F. Boukadi[3], W. Chalgham[4], H. Trabelsi[5]

University of Louisiana, Dept. of Petroleum Engineering, Lafayette LA, USA

Abstract**—** *Eugene Island (EI) 276 fields presents an interesting case study of overpressure caused by uncompacted porosity, in addition to heat. Mechanics of sand deposition, transgressive shale, surrounding faults, overlying shale barriers and underlying salt diapirs have caused temperature anomalies in the P1-sand. Plio-Pleistocene sandstone reservoirs are supplied with mature hydrocarbons by migration of fluids from overpressured shales upwards along an active fault system. The heat carried by climbing fluids and the existence of highly conductive salt diapirs generate strong temperature variances disturbing the entire mini-basin. A COMSOL Multiphysics thermal simulation model has been developed to duplicate temperature variation in well #12, drilled in the proximity of a fault and a salt diapir. Recorded temperatures show a variation in the order of 42 ^{o}F across a shale barrier separating the reservoir from top formation. Heat conduction originating from the salt dome was found to be the dominant heat transfer mechanism, transgressive shale and shale barriers contributed to entrapment and led to overheating.*

Keywords**— Eugine Island, thermal analysis, heat transfer, temperature distribution.**

I. INTRODUCTION

EI330 oil field in the Northern Gulf of Mexico is a nearby giant oil and gas accumulation (Fig. 1), southwest of EI276. It was stated that the field has been the focus of an exceptional interdisciplinary effort to comprehend the changing aspects of an active oil field. The largest Pleistocene oil field in the world [Anderson *et* al., 1994], EI330 is at the staple of a dynamic growth fault system. Over the 30 years since discovery, multiple indications have revealed that hydrocarbons have been migrating along the fault during the recent history and are still flowing. This has been proven by: 1) the presence of hydrocarbon oozes at the sea floor, 2) differences between oil maturity in the multiple reservoirs, and 3) sequential changes in the composition of oils produced over the last 20 years [Anderson *et* al., 1994 and Holland *et* al., 1990]. Identifying the mechanisms of overpressure caused by heat will help direct future drilling and delineation activities in Block 276.

It was stated that unlike seismic traits, formation temperature can be an excellent indicator of long-term fluid circulation. The temperature variation is caused by a combination of possible fluid migration along faults and the presence of heterogeneous structures such as salt diapirs (domes) and transgressive shale, common in the Gulf of Mexico. In this study, we will be utilizing COMSOL to model heat transfer to justify temperature variation in well #12 and better interpret overpressure in P1-sand.

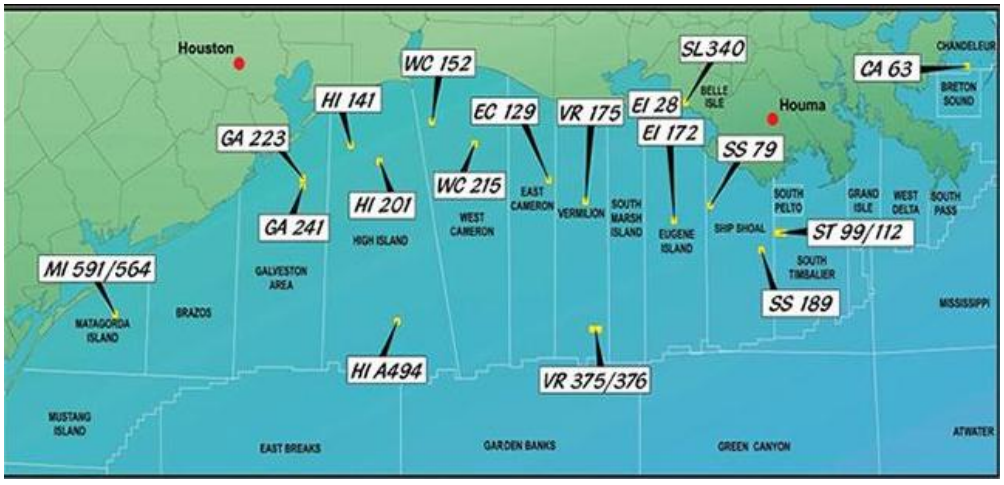

FIG. 1: EUGENE ISLAND FIELD LOCATION

II. GEOLOGICAL SETTINGS

EI276 is offshore St. Mary Parish, Louisiana, 65 miles from shore, under 170 ft of water. Shallowest salt was encountered at a depth of 4962 ft, the deepest salt was met at a depth of 14,150 ft. The deepest well, EI275, is Texaco OCS-G-0988 #4 drilled to a total depth (TD) of 14,495 ft. EI276 field neighbors EI330 lying under 246 ft of water, approximately 170 mi southwest of New Orleans, near the southern edge of the Louisiana Outer Continental Shelf.

The rapid influx of Upper Cretaceous and Lower Tertiary terrigeneous sediments from the ancestral Mississippi delta has mobilized the Jurassic Louann salt, which left a trail of isolated salt dome across the shelf, and formed semicontinuous salt uplifts under the slope of the Gulf Coast margin [Woodbury *et* al., 1973]. EI330 study area is made of nine property blocks located at the transition between these two salt provinces [Holland et al., 1990], with two salt diapirs underneath the South-East and the North-West corners of the study area. The Tertiary and Quaternary sediments overlying the salt define three main facies representative of the normal evolution of a deltaic system prograding across a continental margin [Selley, 1988; Holland *et* al., 1990, Alexander and Flemings, 1995]: 1) directly over the salt, massive shales and turbidites were deposited in a prodelta environment. 2) They are overlain by a sequence of proximal deltaic sands and transgressive shales deposited during sea-level fluctuations when the delta slope was located nearby. The most productive reservoirs of the field are in this interval [Holland *et* al., 1990]. 3) The uppermost section was deposited after the delta had prograded southward, and is composed of fluvial massive sands. The transitions between the different sedimentation phases were identified in the 3D seismic data by reflectors corresponding to transgressive episodes. Biostratigraphic markers Cristellaria "S" (Cris S) and Small Gephyrocapsa (2) (Sm Gep (2)) [Alexander and Flemings, 1995] define the bottom and the top of the proximal deltaic phase, respectively.

Structurally, the EI276 field is a classic salt-withdrawal shelf minibasin [Alexander and Flemings, 1995]. It is bounded by 4 main fault zones (see Fig. 2). The northern, western and southern boundaries are defined by normal faults, while the eastern border is defined by a fault that developed as extensional compensation during the salt withdrawal to the south. Oil and gas reservoirs are trapped under two rollover anticlines.

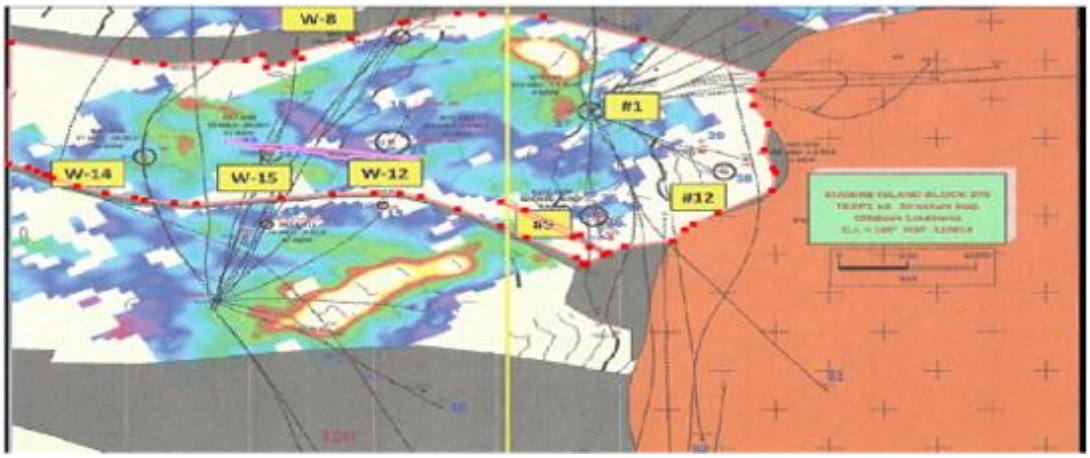

FIGURE 2: EUGENE ISLAND TOP STRUCTURAL MAP

III. TEMPERATURE DISTRIBUTION

Nagihara and Smith [2008] indicated that nearly 600 bottom-hole temperature data from the northern continental shelf of the Gulf of Mexico, each corrected for drilling disturbance, yielded a regional map of geothermal gradient down to approximately 3.7 mi sub–sea floor. Two geographic trends were seen on the map. First, from east to west, the geothermal gradient changes from values between 0.014 and 0.016°F/ft off the Alabama–Mississippi shore to lower values of 0.008 – 0.014°F/ft off eastern Louisiana and to higher values of 0.016 – 0.033°F/ft off western Louisiana through Texas. Second, thermal gradients tend to be lower toward the outer continental shelf (less than 0.0112°F/ft). The authors believe that the observed variations are primarily attributable to the thermal effect of rapid and regionally variable sediment accumulation during the Cenozoic era, which resulted in the occurrence of the geopressured zone in the Texas–Louisiana shelf. In the eastern Louisiana shelf, where accumulation was fastest, sediments down to about 3.7 mi are relatively young (about <15 Ma) and have not had enough time to fully equilibrate with deeper, hotter sediments. That resulted in the low thermal gradient. As the depocenter migrated farther offshore, younger sediments accumulated more in the outer shelf and resulted in an even lower thermal gradient there. However, this mechanism alone cannot explain the fact that geothermal gradients in the

Texas shelf are higher than those in the Alabama shelf, where Cenozoic sedimentation has been much slower. It may be suggested that the contrasting sedimentation history between the Texas and Alabama shelves has resulted in some difference in overall thermal conductivity of sediment, and that the geothermal gradients reflect such difference. However, it is more plausible if additional mechanisms enhance heat flow through sediment in the Texas shelf, such as (1) upward migration of pore fluid expelled from deep, overpressured sands and/or (2) a greater amount of heat released from the igneous basement. Deep sedimentary temperatures in the high-thermal-gradient areas suggest higher risks of hydrogen sulfide occurrence and reservoir quality degradation because of quartz cementation.

Leipper [1954] presented the average outer continental sea surface temperatures for the months of February and August. According to Leipper, the main feature of the average winter pattern is a gradual drop from approximately 75 ^{o}F in the South to an average of 65 ^{o}F in the North, in all parts of the Gulf of Mexico. In the Summer time, Leipper indicated that average temperatures are nearly constant at around 84 ^{o}F. It was also stated [Weatherford, 2009] that sea floor temperature in the Gulf of Mexico at Block 276 depths is at around an average of 60 ^{o}F.

Using well logs from W-4, W-8, W-12, W-15, #1, #9 and #12 in block 276 P1-sand, and an average sea floor temperature of 60 ^{o}F, the temperature gradient taken at depths greater than a shale barrier divide was calculated to be at 1.23 ^{o}F/100 ft (see well log temperature gradient plot in Fig. 3, below). This confirms the theory that a hotter gradient is active in well #12 and any future drilling and delineations have to be planned away from the eastern flank of Block #276, away from the salt diapir.

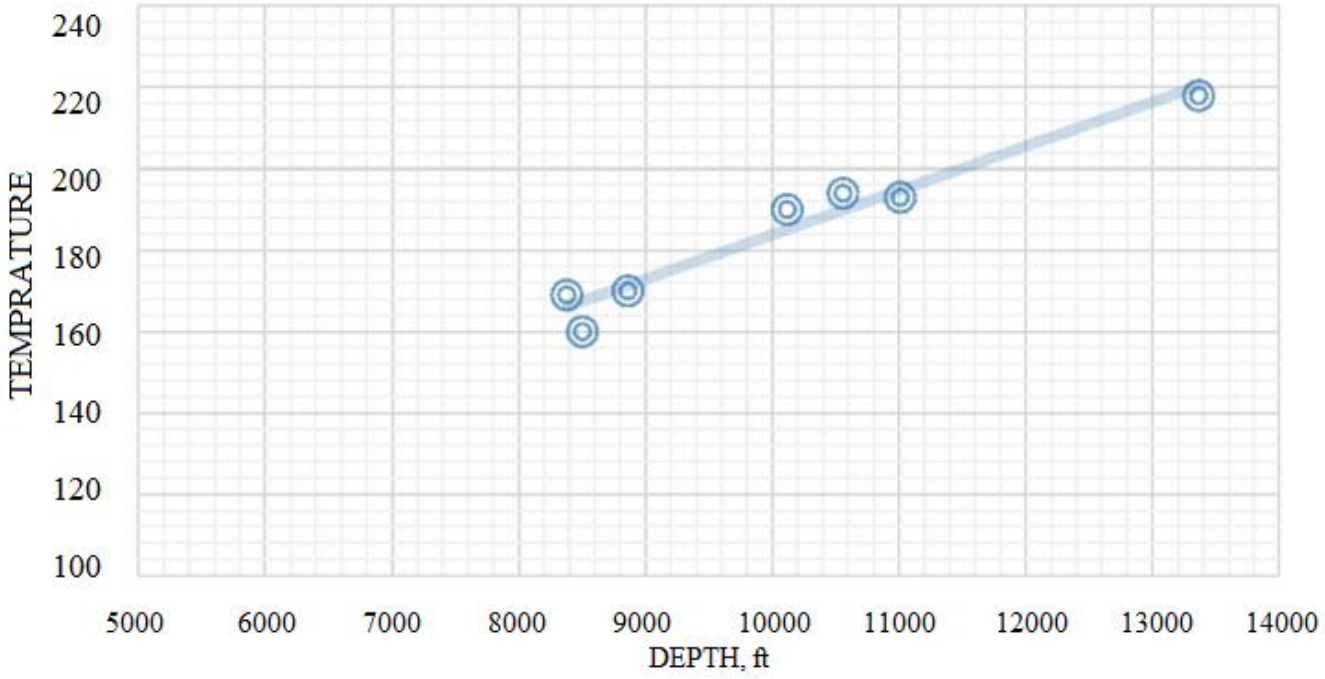

FIGURE 3: TEMPERATURE GRADIENT IN BLOCK 276 P1 SHALY SAND PORTION

Additionally, The P1-sand has seen a resistivity shift at the paleo marker at about 7500 ft [Lane and Macpherson, 1976]. This has also been observed from well testing information (see Fig. 4 below). Temperature has increased from 133 ^{o}F at a true vertical depth sub-sea (TVDSS) of 7573 ft to 165 ^{o}F at 7621 ft in well #12 (the closest well to the salt dome). The shift in temperature indicates that a heat source, transgressive shale, a barrier and obviously oil and gas accumulations, preventing heat dissipation and causing warming, exist. For that matter, resistivity logs from well #12 indicate that a shale barrier exits between the measured depths of 7573 and 7621 ft (see Fig. 5, below); thereby, resulting in heat entrapment.

The same could be said about transgressive shale in P1-sand depths of 7415 to 7680 ft (Fig. 5). The shift in temperature also indicates that a heat source leading to a hotter temperature is located nearby. Just below well #12, a salt diapir is the source of the heat (see top view of a section of Block 276 in Fig. 2, above).

Additionally, the following 3-D view (Fig. 6) also confirms that well #12 is in a hotter zone and that development wells should be planned on the downdip, western flank of the reservoir to prevent drilling hazards and future production problems. According to Forrest et al. [2007], the same phenomenon has been observed in EI292 with a temperature shift at Base Mud Line Depths (BMLD) between 2000 and 4000 feet (see Fig. 7).

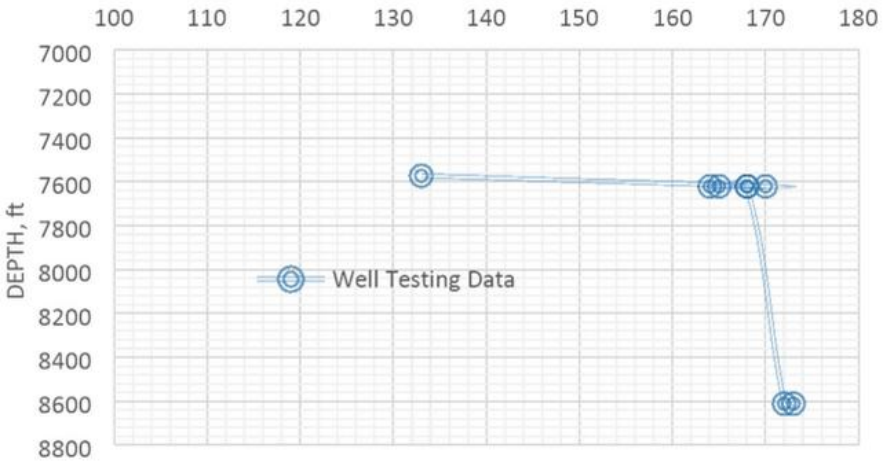

FIGURE 4: TEMPERATURE PROFILE REVERSAL AT BOTTOM OF WELL #12 IN BLOCK 276 P1-SAND

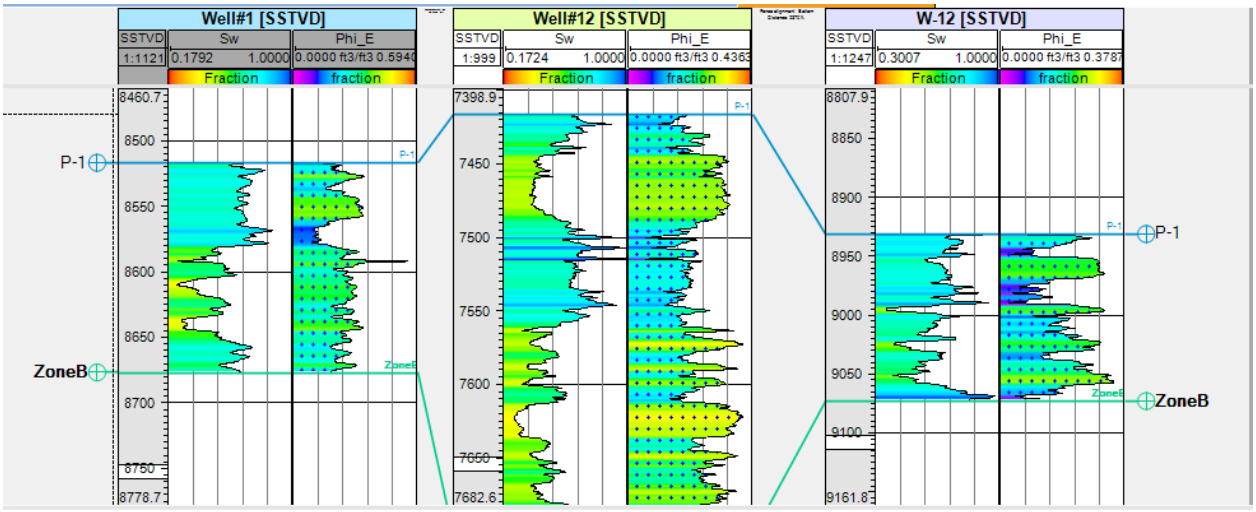

FIGURE 5: TRANSGRESSIVE SHALE AT DEPTHS (7415-7680 FT) CAUSING HEAT ENTRAPMENT

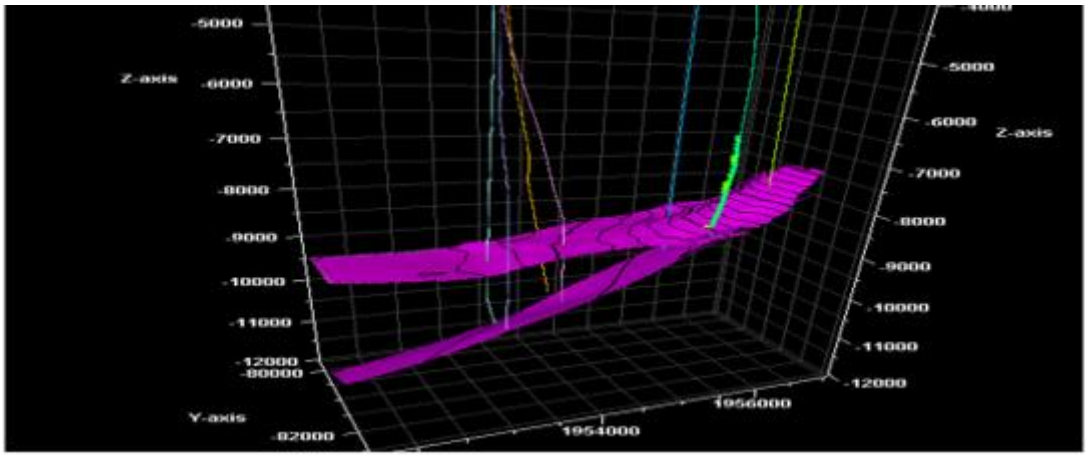

FIGURE 6: WELL #12 (FAR RIGHT, UPSTRUCTURE) CLOSE TO THE SALT DIAPIR

In their study of geothermal gradients and subsurface temperatures in the Northern Gulf of Mexico, the authors calculated geothermal gradients for 1131 fields and wells, and a map has been prepared showing the below-mudline depth to the 300°F subsurface isotherm over the northern Gulf of Mexico. The authors stated that since the 300°F isotherm values are a direct reflection of thermal gradient, thermal conductivity, and heat flow, the map may be considered as a portrayal of subsurface temperature distribution. They noted that based on interpreted vertical and horizontal temperature patterns, the northern Gulf can be subdivided into six thermal domains. The authors added that the moderately high temperatures and a pattern of isotherm contours related to salt features characterize the Louisiana shelf domain, in particular. To model temperature

discrepancy around well #12, COMSOL Multiphysics was used to conduct thermal analysis and validate the theory of heat entrapment.

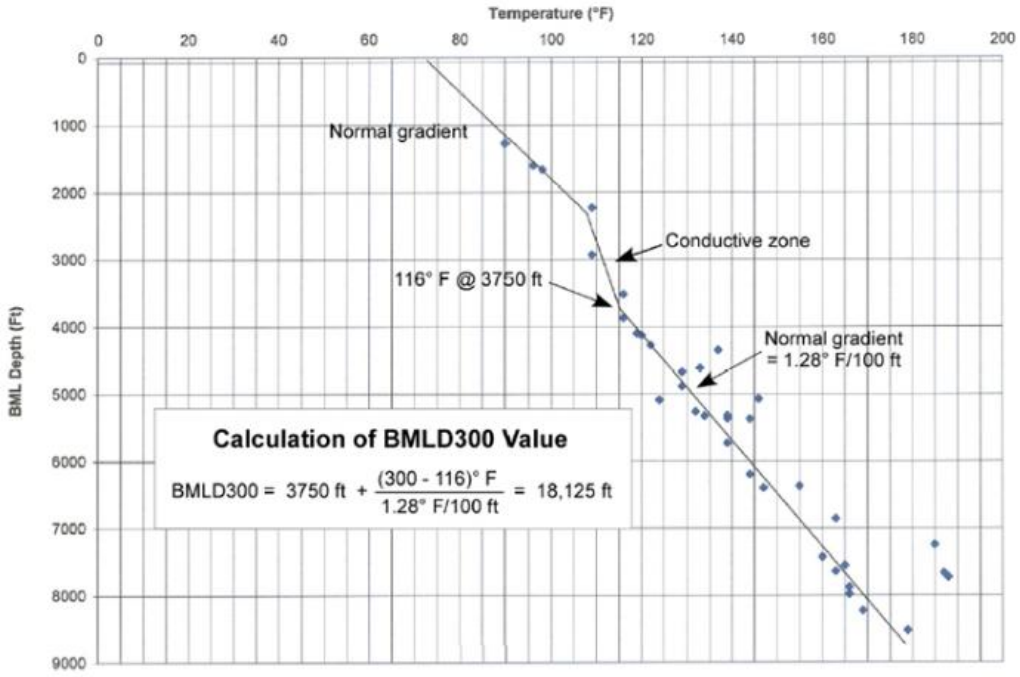

FIGURE 7: AVERAGE TEMPERATURE-DEPTH PLOT OF SANDS IN EI292 FIELD. DATA FROM MMS ATLAS OF NORTHERN GULF OF MEXICO GAS AND OIL SANDS [2001]

IV. HEAT TRANSFER IN SEDIMENTARY BASINS

Heat transfer in sedimentary formations can be described by the following equation of conservation of energy:

$$\int_V \frac{\partial(\rho CT)}{\partial t} dV = \int_S \lambda \nabla T \, dS - \int_S \rho_f C_f T V_d dS + \int_V H dV \tag{1}$$

where V and S are, respectively, the volume and the external surface of an arbitrary unit of sediments and dS is the normal to S. The left side of the equation is the variation of internal energy which is a function of bulk density (ρ), specific heat of the sediments (C), and temperature (T). The first term on the right symbolizes heat transfer by conduction defined by Fourier's law and proportional to thermal conductivity of the minerals (λ) and to the temperature gradient (∇T) across the surface S. This term is typically the dominant heat transfer component in sedimentary basins [Rybach, 1981] causing strong variance in the presence of geological bodies of high thermal conductivity like salt despairs [Mello *et* al., 1994]. The second term represents the heat carried by fluids of specific heat (C_f) and density(ρ_f) flowing with Darcy velocity(V_d). It is assumed that the pore space is fluid-saturated and that the volumetric flow rate can be expressed using Darcy's law for single phase fluid flow, $V_d = -\frac{k}{\mu}[\nabla P - \rho_f g]$ where, ∇P is the pressure gradient, k, the permeability of the sediments, μ, the dynamic viscosity of the fluid and g, the acceleration of gravity. The last term in the heat transfer equation (1) is the heat created by eventual sources of volumetric strength H.

To simulate heat transfer, we assume that the temperature distribution is continuous and varies smoothly at grid block's scale. Equation (1) is discretized as follows:

$$\frac{\partial(\rho CT)}{\partial t} = \nabla(\lambda \nabla T) - \nabla(\rho_f C_f T V_d) + H \tag{2}$$

4.1 Heat sources

In this study, it was considered that the heat flux has been generated by the combined dominant effects of (1) radiogenic heat (2) heat produced by chemical reactions and (3) sedimentation. The radiogenic heat produced by decay of radioactive

isotopes of Potassium, Thorium and Uranium, the heat produced by chemical reactions (like diagenesis and hydrocarbon generation), and also the effect of sedimentation was discarded.

Sedimentation is active and taking place at a rate of 1.0 mm/year. However, salt movement in the Eugene Island area has stopped about 1.5 million years ago. It was also stated that temperature change over the last 100,000 years is less than 0.2°C, almost in steady state after stoppage of salt movement, and is practically constant at present time [Alexander and Flemings, 1995]. Moreover, we will consider that fluid flow via faults into the reservoir is extremely small; thereby, it can be assumed that V_d is negligible. As such, Equation (2) reduces to the following:

$$\frac{\partial(\rho CT)}{\partial t} = \nabla(\lambda \nabla T) \tag{3}$$

4.2 Analysis of temperature distribution around well #12

The reservoir under study consists of three distinct regions i) a clean sand at the top of the reservoir, ii) a shaly sand in the bottom portion, and iii) a shale barrier, sandwiched between the two (see Fig. 8, below). Fig. 8 also describes the model that will be used to predict the thermal variation along the depth of P1-sand. The three regions are characterized by lower temperatures for thin sand-rich formations, whereas, higher temperatures distinguish thick shaly formations, since sand-rich sections have a higher thermal conductivity.

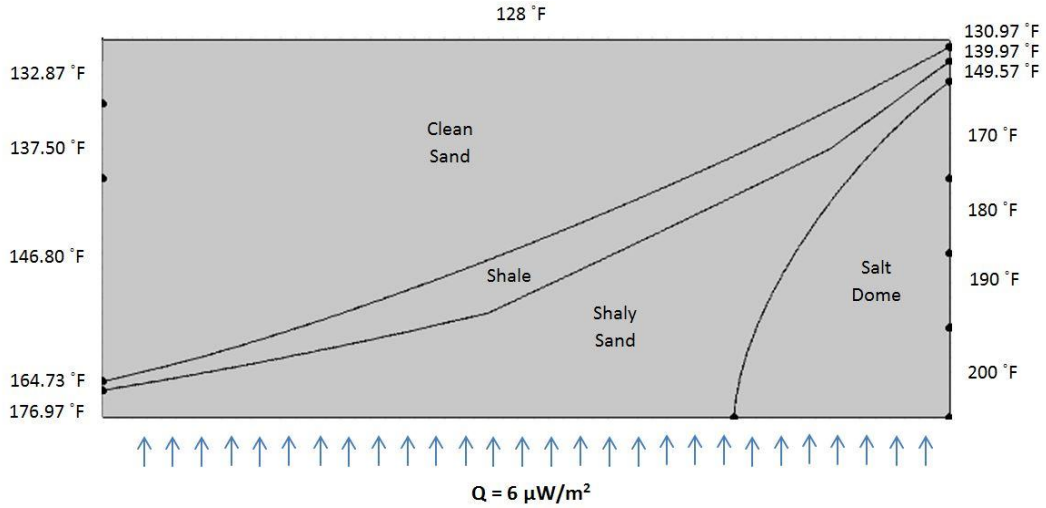

FIGURE 8: SCHEMATIC OF MODEL USED FOR COMSOL MUTIPHYSICS SIMULATION

It was assumed that a uniform heat flow from the basement (salt dome) through a sequence of shaly sand, shale, then clean sand formations. The thick shaly sand on top of the salt dome maintains higher temperatures. A drastic temperature drop, across the shale and into the clean-rich sand, is in the neighborhood of 43 ^{o}F. Temperatures at the outer eastern and western boundaries, delimited by faults, have been set to vary at a constant temperature gradient. It was stated that high thermal conductivity of the salt compared to the surrounding sediments (4-6 W/mK vs. 1-3 W/mK, [Mello et al., 1994]) and the high amplitude of salt topography, described by Anderson et al. [1994] as the most rugged topography on earth can generate significant temperature anomalies [Mello et al., 1994].

Coelho et al. [1996] confirmed that presence of oil and gas decreases thermal conductivity, leading to thermal draping that increases temperature underneath reservoirs. The authors indicated that influence of hydrocarbons could cause a positive temperature difference, as high as 15 ^{o}C below the main reservoirs, and could explain by itself the recorded differences. However, using their theory, it was found that such blanketing would require about 60% of gas distributed uniformly in a pore space with an average porosity of about 40 % between 1,000 and 2,000 mbsf (meter below sea floor, also known as TVDSS). This does not represent P1-sand, deeper and mostly oil-saturated.

V. THERMAL ANALYSIS

Heat generated by conduction is the dominant component in Equation (1). It was assumed that conduction governs heat flow across the faults (surrounding the reservoir) and dominates the influence of the salt dome. Average values for salt conductivity and density and specific heat of the fluids are λ=6 W/mK, ρ_f=1000 kg/m^3 and C_f=1.5 J/Kkg^3, respectively.

5.1 Numerical Analysis

Using a control volume fixed with regard to the shallowest horizon of the P1-sand (see Fig. 8).

In permanent regime, this can be written as:

$$\int_S \lambda \nabla T dS - \int_S \rho_r C_r T U dS = 0 \tag{4}$$

where U represents type of sediment (whether salt, clean sand, shaly sand or shale), ρ_r and C_r are the density and specific heat of the sediment. Tables in the Appendix summarize property values used in the analysis of temperature distribution, vertically in the well #12 area of interest. Using a finite difference formulation for a surface S with n gridblocks, each having the same dimensions Δx and Δz, one can write the following:

$$\sum_{i=b,t,e,w} k_i S_i \frac{(T_i - T_{i-1})}{d_i} + \sum_{i=b,t,e,w} \rho_r C_r U \Delta x \Delta z \left[\frac{(T_t + T_{i-1})}{2} - \frac{(T_b + T_{i-1})}{2}\right] = 0 \tag{5}$$

where the subscript i represents direction and b, t, e, and w all represent bottom, top, east and west bounds of two neighboring blocks i and $i-1$. The terms d_i and S_i are the grid dimensions along and surface orthogonal to direction, d, respectively. Thermal conductivity between two neighboring blocks is the harmonic "in series" average of the thermal conductivity of i and $i-1$:

$$k_i = \frac{2\lambda_i \lambda_{i-1}}{\lambda_i + \lambda_{i-1}} \tag{6}$$

The centered space over-relaxation method [Press, 1994] that is used to solve Equation (5) is an iterative algorithm where an initial temperature value is attributed to all nodes at initial step (T^0). Temperature T^{n+1} at step $(n+1)$ for any node is calculated from values of previous step (n) at adjacent nodes, until reaching a convergence limit, ε. In the control unit, where node dimensions are $\Delta x\, \Delta y$ and Δz, the recurrent formula is:

$$T_i^{n+1} = (1-\alpha) T_i^n + \beta \left[\Delta x \Delta y (T_t^n k_t + T_b^n k_b + \gamma (T_t^n - T_b^n)) + \Delta y \Delta z (T_e^n k_e + T_w^n k_w)\right] \tag{7}$$

with, $\beta = \frac{\alpha}{\Delta x \Delta y (k_t + k_b) + \Delta y \Delta z (k_e + k_w)}$ and $\gamma = \frac{U \rho v C}{2}$

where, α is the over-relaxation coefficient taken between 1.0 and 2.0 for unconditional convergence [Press, 1994].

VI. RESULTS AND DISCUSSION

In the developed model, four different types of formation with specific attributes were used. These correspond to the main facies associated with the development of the minibasin, from bottom up: the salt diapir (1) overlain by sand and transgressive shale (2) a shale barrier (3), and an uppermost section composed of clean sands (4), as depicted in Fig. 8 above.

Neither fine gridding nor a complete reproduction was attempted; the idea was to develop a better understanding of heat dissipation in block EI276.

The initial and boundary conditions were chosen to be representative of recorded well testing bottomhole temperatures in well #1 and #12, both sit on the top of the semi-anticline on the eastern boundary portion of the reservoir in the vicinity of faults and the salt dome. Temperature at the top of the control surface was extrapolated to 128 ^{o}F, using a cold temperature gradient of 1.0 ^{o}F/100 ft (clean sand). A null heat flux across the lateral boundaries (null horizontal gradients) was used.

Temperatures on the eastern and western fault boundaries were extrapolated from obtained data using observed gradients across the different formations. These are 1.0 ^{o}F/100 ft in clean sand and 1.23 ^{o}F/100 ft in the shaly deeper sand beds, respectively. A uniform vertical heat flow at the bottom boundary (60 $\mu W/m^2$, from Anderson *et* al. [1991]) was also utilized to simulate salt dome conduction.

COMSOL results showed a 41 ^{o}F temperature anomaly between temperatures in Well #12 producing from sand and transgressive shale, located in the vicinity of a salt dome, and a shallower well #1 producing from clean sand and more remote from the conductive salt dome source. The influence of salt dome is significant and conduction played a major role in

temperature rise in well #12. Transgressive shale, shale, oil and gas have also contributed to temperature entrapment (Fig. 9). It can be observed that shale acted like a thermal barrier where there are two distinctive thermal regions (above and below shale layer) that exhibit various temperature gradients (1.0 and 1.23 ^{o}F/100 ft).

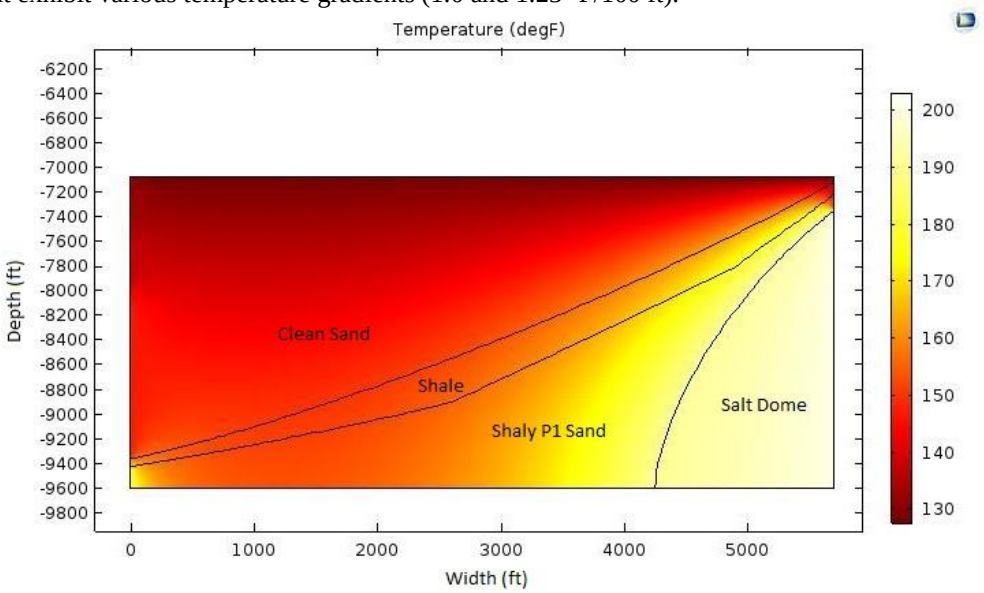

FIGURE 9: HEAT TRANSFER SIMULATION CONTROL VOLUME

The isothermal contours lines shown in Fig. 10 clearly show a temperature discrepancy in the salt dome and across the shale barrier. The observed temperature drop across the shale barrier of 43 ^{o}F was reproduced with a calculated simulation drop of 41 ^{o}F. That corresponds to an absolute error of 5.7% indicating that the simulation results agree with the reported data and consolidated the hypothesis that salt domes are the major source of heat and that the dominant mechanism of heat transfer in the Eugene Island area is by conduction.

A sensitivity analysis on heat influx magnitude and dome temperature was performed. COMSOL reproduction of observed data was achieved for a heat influx value of 6.0 $\mu W/m^2$ and a dome temperature gradient of 7.5 ^{o}F/100 ft on the eastern side of the structure. A 1.6 ^{o}F/100 ft on the western side of the structure was utilized in the clean sand portion of the P1-sand. Another temperature gradient of 2.2 ^{o}F/100 ft along the shaly-sand portion (resulting in a high temperature concentration at the left bottom corner of the control volume) was used to match the observed temperature profile. Figure 8 is an illustration of the sensitivity analysis parameters.

Pertinent modeling data are all summarized Tables 1 to 4 in Appendix A.

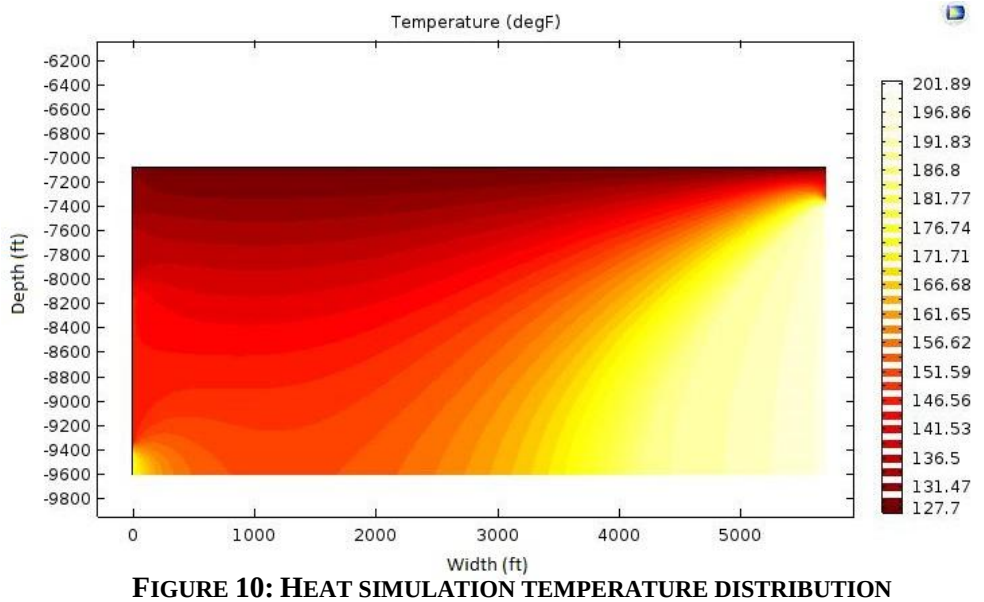

FIGURE 10: HEAT SIMULATION TEMPERATURE DISTRIBUTION

VII. CONCLUSIONS

A thermal analysis of the vicinity of well #12 was conducted using COMSOL multiphysics to predict temperature variation along the P1-sand depth. The developed model validated the variation in temperature between cold clean and hotter shaly sands and predicted a temperature contrast of 41 ^{o}F across the shale barrier. This is in agreement with the observed temperature departure of 43 ^{o}F. The temperature variation indicated that salt diapirs transferred heat by conduction to the reservoir, increased temperature around nearby wells. COMSOL simulation results also confirmed that shale acted as a thermal barrier and helped retaining heat in the shaly sand.

REFERENCES

[1] L. L. Alexander, P.B. Flemings, "Geologic evolution of a Plio-Pleistocene salt withdrawal Mini-Basin: Block 330, Eugene Island," South Addition, Offshore Louisiana, AAPG Bull., 79(12), 1995, pp. 1737-1756.

[2] R. N. Anderson, P. B. Flemings, S. Losh, J. Austin, R. Woodhams, "Gulf of Mexico Growth fault drilled, seen as oil, gas migration pathway," Oil and Gas Journal, June 6, 1994, pp. 97-103.

[3] D. Coelho, A. Erendi, L. M. Cathles, "Temperature, pressure and fluid flow modelling in Block 330, South Eugene Island using 2D and 3D finite element algorithms," Annual Meeting Abstracts - AAPG and SEPM, v. 5, 1996, pp. 28.

[4] J. Forrest, E. Marcucci, P. Scott, "Geothermal gradients and subsurface temperatures in the Northern Gulf of Mexico," GCAGS Transactions, v. 55, 2007, pp. 233-248.

[5] R. A. Lane, L. A. Macpherson, "A review of geopressure Evaluation from well logs – Louisiana Gulf Coast," Journal of Petroleum Technology, 1976, pp. 963-971.

[6] D. S. Holland, J. B. Leedy, D. R. Lammlein, "Eugene Island Block 330 field, offshore Louisiana, in Beaumont, E.A., and Foster, N. H., compilers, Structural traps III, tectonic fold and fault traps," AAPG Treatise of Petroleum Geology Atlas of Oil and Gas Fields: 1990, pp. 103-143.

[7] D. F. Leipper, "Physical oceanography of the Gulf of Mexico, Fishery Bull., 55(89): 1954, pp. 119-138.

[8] S. Nagihara, M. A. Smith, "Regional overview of deep sedimentary thermal gradients of the geopressured zone of the Texas–Louisiana continental shelf,: AAPG Bull. 92, 2008, pp. 1-14.

[9] U. T. Mello, R. N. Anderson, G. D. Carner, "Salt restrains maturation in subsalt plays, Oil and Gas Journal, 31, 1994, pp. 101-107.

[10] W. H. Press, S. A. Teukolsky, W. T. Vetterling, B. P. Flannery, "Numerical recipes in C: the art of scientific computing" 2nd edition, Cambridge University Press, New York, 1992.

[11] L. Rybach, "Geothermal Systems, Conductive Heat Flow, in Geothermal Systems: principles and case histories, L. Rybach and L.J.P. Muffler, John Wiley and Sons, Ltd, 1981.

[12] R. C. Selley, "Applied Sedimentology. xii + 446 pp. London: Academic Press, 1988.

[13] H. O. Woodbury, I. B. Murray, P. J. Pickford, W. H. Akers, "Pliocene and Pleistocene depocenters, outer continental shelf. Louisiana and Texas: *AAPG Bull.*, 57, 1973, pp. 2428-2439.

Appendix A
Materials properties used in COMSOL multiphysics.

TABLE 1
MATERIAL PROPERTIES OF SHALE BARRIER

Material Contents

Property	Name	Value	Unit	Property group
Thermal conductivity	k	1.043633...	W/(m·K)	Basic
Density	rho	2322.677...	kg/m^3	Basic
Heat capacity at constant pressu...	Cp	803.8656	J/(kg·K)	Basic
Ratio of specific heats	gamma	1	1	Basic

TABLE 2
MATERIAL PROPERTIES OF P1-SAND

Material Contents

Property	Name	Value	Unit	Property group
Thermal conductivity	k	0.95	W/(m·K)	Basic
Heat capacity at constant pressu...	Cp	766.1844	J/(kg·K)	Basic
Density	rho	2178.511	kg/m^3	Basic
Ratio of specific heats	gamma	1	1	Basic

TABLE 3
MATERIAL PROPERTIES OF SALT

Material Contents

Property	Name	Value	Unit	Property group
Thermal conductivity	k	6	W/(m·K)	Basic
Heat capacity at constant pressu...	Cp	880	J/(kg·K)	Basic
Density	rho	2200	kg/m^3	Basic
TD	TD	1.99e-9		Basic
Ratio of specific heats	gamma	1	1	Basic

TABLE 4
MATERIAL PROPERTIES OF CLEAN SAND

Material Contents

	Property	Name	Value	Unit	Property group
☑	Heat capacity at constant pressu...	Cp	773.72	J/(kg·K)	Basic
☑	Thermal conductivity	k	0.91	W/(m·K)	Basic
☑	Density	rho	2274.62	kg/m^3	Basic
	Ratio of specific heats	gamma	1	1	Basic